Proceedings of Conference Medical Imaging 2001 : Image Processing (SPIE #4322), San Diego, 19-22 Février 2001, p. 1218-1225

Procedure to detect anatomical structures in optical fundus images

L. Gagnon[*a], M. Lalonde[*a], M. Beaulieu[*a], M.-C. Boucher[**b]
[a]Computer Research Institute of Montreal; [b]Dept. Of Ophthalmology, Maisonneuve-Rosemont Hospital

ABSTRACT

We present an overview of the design and test of an image processing procedure for detecting all important anatomical structures in color fundus images. These structures are the optic disk, the macula and the retinal network. The algorithm proceeds through five main steps: (1) automatic mask generation using pixels value statistics and color threshold, (2) visual image quality assessment using histogram matching and Canny edge distribution modeling, (3) optic disk localization using pyramidal decomposition, Hausdorff-based template matching and confidence assignment, (4) macula localization using pyramidal decomposition and (5) vessel network tracking using recursive dual edge tracking and connectivity recovering. The procedure has been tested on a database of about 40 color fundus images acquired from a digital non-mydriatic fundus camera. The database is composed of images of various types (macula- and optic disk-centered) and of various visual quality (with or without abnormal bright or dark regions, blurred, etc).

Keywords: Ophthalmic image analysis, medical imaging, anatomical structures

1. INTRODUCTION

The aim of this paper is to present an overview of the design and test results of a practical image processing procedure to detect all important anatomical structures in color retinal images. These structures are the Optic Disk (OD), the macula (fovea) and the retinal network.

Detection of anatomical structures is important in many ways:

- Segmenting the OD is a key pre-processing element in many algorithms designed for automatic extraction of anatomical structures and detection of retinal lesions. This is notably the case for vessel tree extraction, for which large vessels located in the vicinity of the OD can serve as seeds for vessel tracking procedures [1,2]. Masking the OD also helps reducing bias regarding retinopathy-related lesions detection [3].
- Macula encircling helps establishing statistics regarding lesions position for disease gradation. The relatively constant distance between the OD and the macula center can be used as *a priori* knowledge to help positioning the macula [4].
- Vessel tracking provides a map of the retinal vessels of the eye, from which a reference frame may be derived that can ease the process of positioning other fundus objects and lesions with respect to a natural "coordinates systems". Vascular network also allows the localization of stable anchor points (such as bifurcation) needed for image registration [5] as well as the characterization of veins associated to specific pathology like venous beading (veins tortuosity that reflects the progress of diabetic retinopathy) [6,7]. Finally, vessel detection turns out to be helpful to other recognition algorithms that requests the removal of the vascular network [3,5].

As depicted on Figure 1, our procedure follows five main steps: (1) automatic mask generation to avoid processing of the black border in the images, (2) image quality assessment, to reject bad quality images, (3) optic disk localization to assist in the (4) macula localization and (5) vessel network tracking (also assisted by the OD detection step). The procedure implies the use of various image processing tools such as histogram matching, pyramidal representation, edge detection, Hausdorff distance, etc. The procedure has been tested on a database of 40 color fundus images acquired from a digital low-resolution (20 microns/pixel) non-mydriatic fundus camera (Canon CR6-45NM). The database is composed of images of various types (macula- and optic disk-centered) and of various visual quality (with or without abnormal bright or dark regions, blurred, etc). The procedure shows robustness to all of these image characteristics (see Ref. [3,4,8-10] for more details).

*langis.gagnon@crim.ca; phone 514-840-1235; fax 514-840-1244; http://www.crim.ca; Computer Research Institute of Montreal, 550 Sherbrooke Street West, Suite 100, Montréal, QC, Canada, H3A 1B9; **Maisonneuve-Rosemont Hospital, 5689 Boulevard Rosemont, Montreal, QC, Canada, H1T 2H1

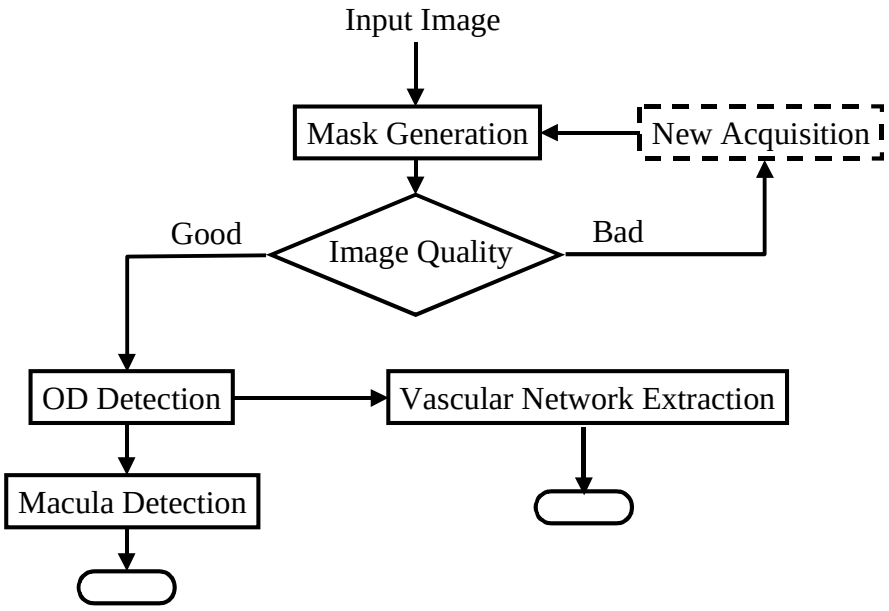

Figure 1: Block diagram of the procedure

The paper is organized according to the application order of the various modules: Section 2 reviews the mask generation algorithm, Section 3 is about the image quality assessment, OD and macula detection are described in Section 4 and 5 respectively, followed by the extraction of the retinal network in Section 6. Finally, conclusion and future works are mentioned in Section 7. More technical details can be found in Refs. [3,4,8-10].

2. MASK GENERATION

Mask generation aims at labeling pixels belonging to the fundus Region Of Interest (ROI) in the entire image. Pixels outside that ROI are those belonging to the dark surrounding region in the image. Those pixels are not strictly dark (0 intensity value) and the need to discard them for subsequent processing stages is necessary.

The mask generation uses pixel value statistics outside the ROI of the fundus image. Statistics are calculated for each color bands of the image followed by a 4-sigma thresholding with a free parameter empirically chosen such that pixels with intensity value above that threshold are considered to belong to the ROI. Results for all bands are combined through logical operations and region connectivity test in order to identify the largest common connected mask (due to different color response of the camera, ROI size is not always the same for each band).

The algorithm is robust enough to allow automatic mask generation on images of low visual quality, which is the principal issue in this step. Figure 2 shows an example of mask generation on a low visual quality image. All images of our dataset were correctly masked with this process.

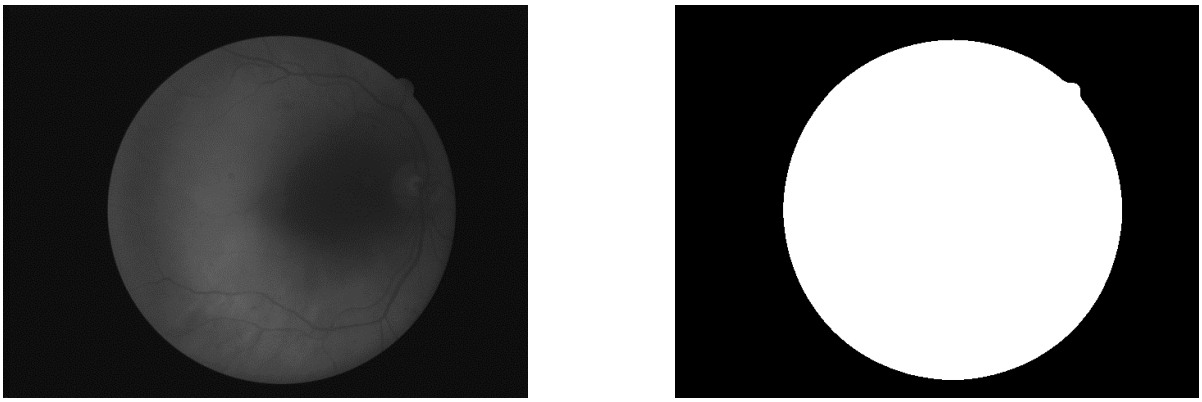

Figure 2: Example of mask generation

3. IMAGE QUALITY ASSESSMENT

Although noise is kept to a minimal level in medical CCD cameras, a number of factors may lead to fundus images of low visual quality. For instance, patient's eye might be blinking during image acquisition, so eyelashes or eyelid may be imaged during the acquisition process. Also, patient might move his head during the examination which might result in (1) out-of-focus images, (2) presence of a part of the iris in the image or (3) darkening the image because of a badly illuminated retina.

Figure 3 gives examples of quality assessments for a good (top-left), fair (top-right) and bad (bottom) quality images, as evaluated by a medical expert. The fair image exhibits eyelashes and darker regions than for good quality images. The bad quality image is so because of the blurring and the dark region around the macula.

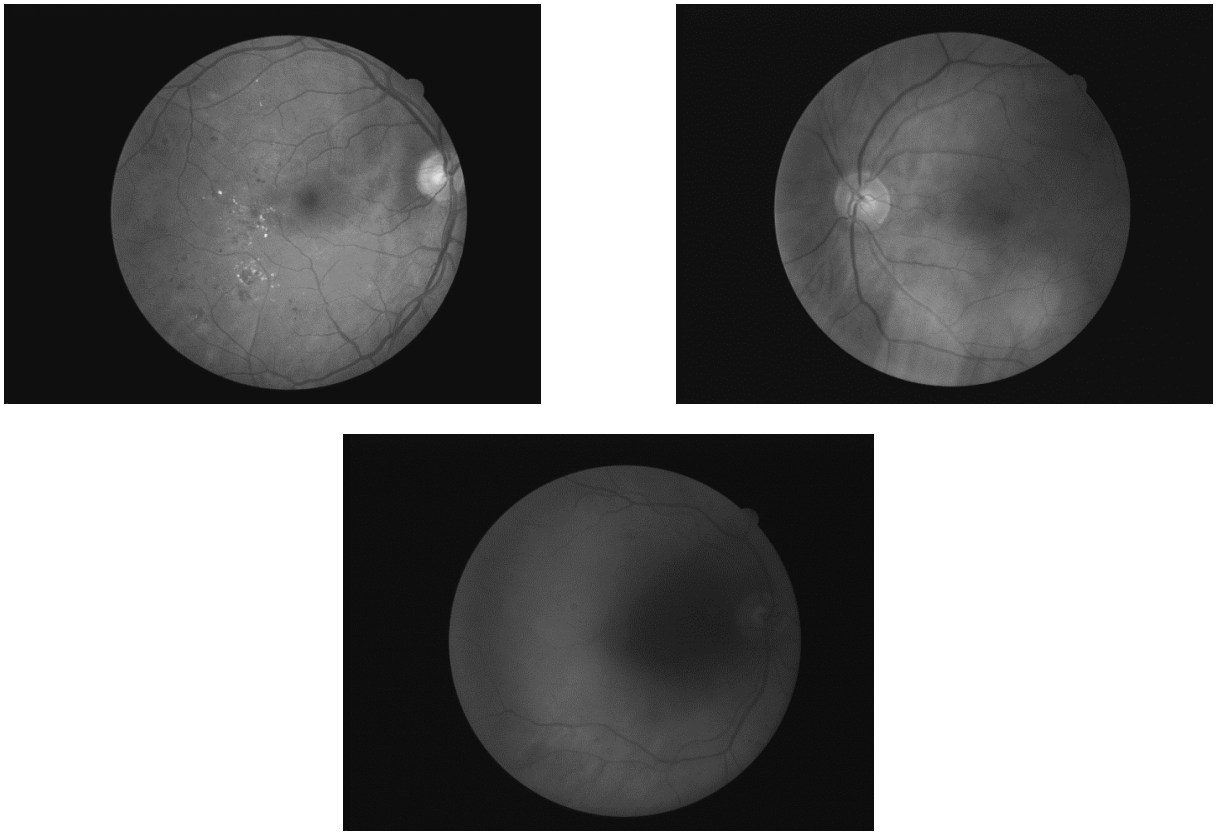

Figure 3: Examples of image quality assessments for a good (top-left), fair (top-right) and bad (bottom) quality images

The image quality assessment module follows a model-based approach that uses model histograms for the pixel and edge value distributions [8]. Our approach is generally similar to that of Lee and Wang [11] in the sense that a model of what is a good image is defined using a set of images of good quality. However, the model itself is different and stems from observations on the characteristics of good and bad images. Two criteria have been retained that focus on:

1. the distribution of the edge magnitudes in the image,
2. the "local" distribution of the pixel intensity

For the pixel value distribution, homogeneous regions are isolated in the image and their mean intensity are compared with a mean model image. Combining the two measures provides a simple way to discriminate between visually good, fair and bad visual quality images. For the edge value distribution, we perform a chi-squared-type histogram matching with a model histogram.

Figure 4 shows the separability of the three quality classes (good, fair and bad) according to our procedure. Among the 40 images in the data set, only 1 good quality image ends up in the bad quality cluster.

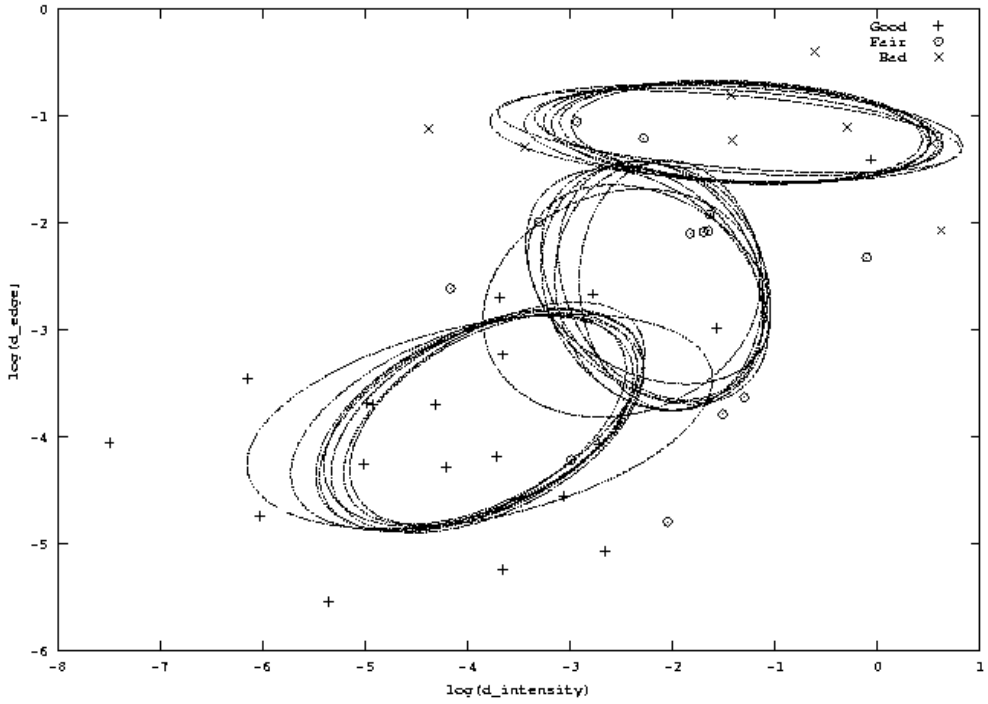

Figure 4: Separability of the three quality classes (good, fair and bad) according to our models for high frequency content and brightness distribution

4. OPTIC DISK DETECTION

Our approach for OD detection attempts to respond to three user-specific and computational requirements:

- robustness to the variable appearance of OD's (intensity, color and contour definition for macula-centered and OD-centered images),
- detection performance above 90%, and
- short computation time.

Furthermore, the algorithm design relies on three assumptions. The first pertains to the image acquisition. Since acquisition of ophthalmic images usually follows a fixed protocol, some information about the retina and its structures can be deduced

and exploited. The ophthalmologist knows which eye (left/right) is being imaged and whether the image is centered on the macula or the OD. This *a priori* information should be exploited in order to guide the search for the OD in a specific portion of the image. The second assumption comes from the observation that the OD represents a bright region (but not necessarily the brightest) in an ophthalmic image of good quality. The last assumption relates to the form of the OD, which always appears approximately circular. The method we propose is decomposed into two stages:

- OD tracking through a pyramidal decomposition, and
- OD contour search technique based on the Hausdorff distance

The global OD region is found by means of a multi-scale analysis (pyramidal approach) using a simple Haar-based wavelet transform. The brightest pixel that appears in a coarse resolution image (at an appropriate resolution level depending on the initial image resolution and the OD average dimension) is assumed to be part of the OD. This global OD localization serves as the starting point for a more accurate OD localization obtained from a template-based matching that uses the Hausdorff distance measure on a binary image of the most intense Canny edges. These intense edges are the ones that pass a intensity thresholding test based on a Rayleigh distribution model of the edge pixels intensity.

Each stage generates a set of hypotheses. These hypotheses are analyzed and combined to provide the best solution.

The approach has been tested against a database of 40 images of various visual quality and retina pigmentation, as well as of normal and small pupils [9]. An average error of 7% on OD center positioning is reached with no false detection. In addition, a Dempster-Shafer confidence level [for instance, see Ref. 12 and references therein] is associated to the final detection that indicates the level of difficulty the detector has to identify the OD position and shape.

Figure 5 gives examples of OD detection on good and bad visual quality images.

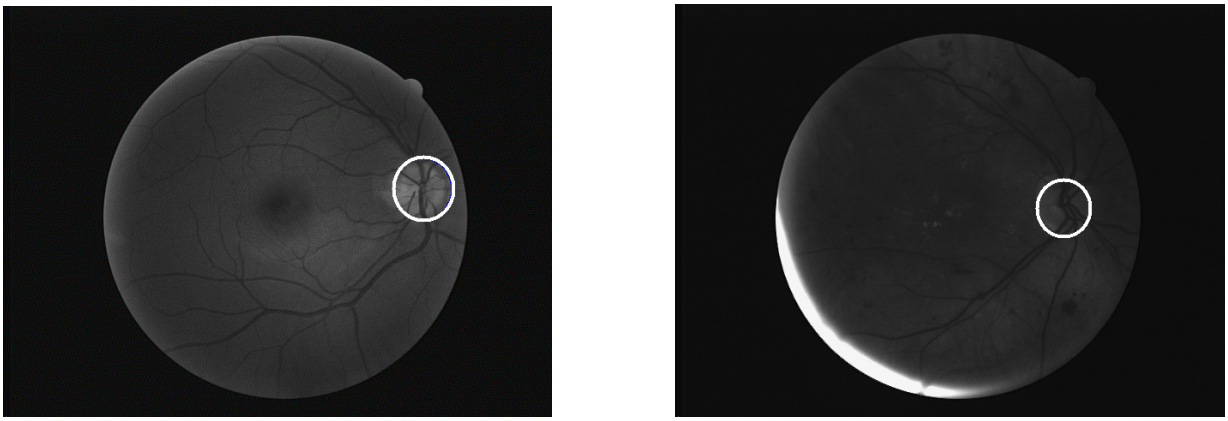

Figure 5: Examples of OD detection on good (left) and bad (right) quality images

5. MACULA DETECTION

Once the OD is detected, the macula is localized by finding the darkest pixel in the coarse resolution image following *a priori* geometric criteria based on the eye's anatomy (macula position and distance with respect to the OD is relatively constant). This darkest pixel in the coarse resolution image corresponds to the region occupied by the macula in the original image. The exact center of the macula is then found by searching in the vicinity for the darkest pixel on the original fine resolution image. A circle with a diameter equals to twice the OD diameter is then drawn around that point.

Figure 6 gives examples of macula detection following an OD detection for the same images as in Figure 5. A success rate of about 95% has been reached with this approach on the 40 images of our image dataset [4].

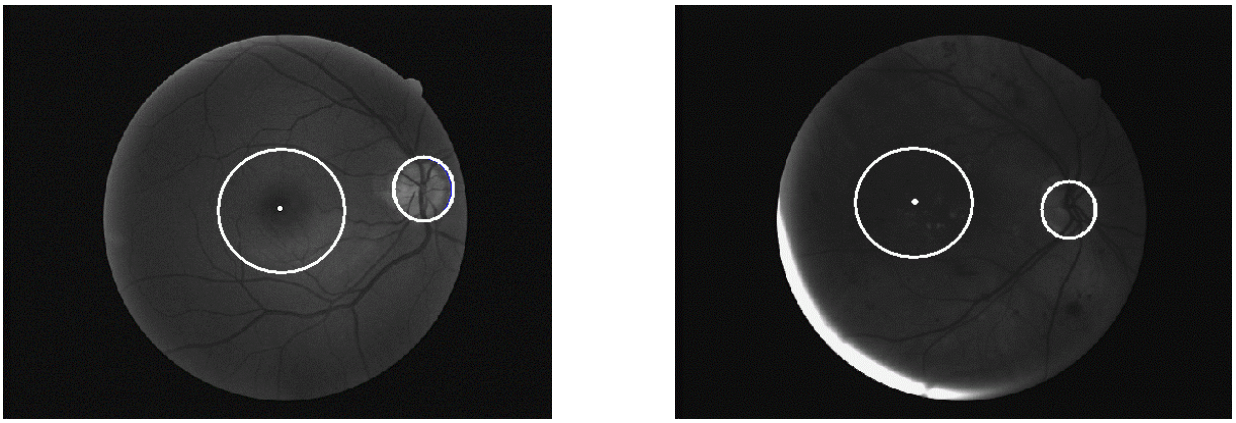

Figure 6: Example of macula detection following OD positioning for the same images as in Figure 5

6. VASCULAR NETWORK DETECTION

The vessel detection module is designed to track the borders of a vessel sequentially [10]. The vessel tracking algorithm is initiated on the border of the OD and uses the image edge map as computed by the Canny edge operator. Tracking proceeds by following an edge line (which coincides with a vein border) while monitoring the connectivity of its twin border (Figure 7). Breaks in the connectivity trigger the creation of seeds that serve as extra starting points for future tracking. Seed creation allows the algorithm to handle bifurcation (a key issue in vessel tracking) and to jump over broken or missing edges.

The algorithm is designed to track the borders of a vessel, following one border at a time while registering the presence of the twin border, until one of the following events occurs: 1) the end of the line is reached, or 2) a junction is met (since the algorithm cannot privilege one direction, it stops). As a consequence, a piece of vessel is analyzed twice, and both analyses should be in agreement. The dual tracking process improves the quality of recognition and ensures that bifurcation are handled properly. The ability of the algorithm to jump over gaps and go beyond bifurcation is provided by an automatic seed generation mechanism that analyses some properties of the twin points and creates new starting points (called seeds) for subsequent tracking according to rules such as connectivity between twin points (Figure 7).

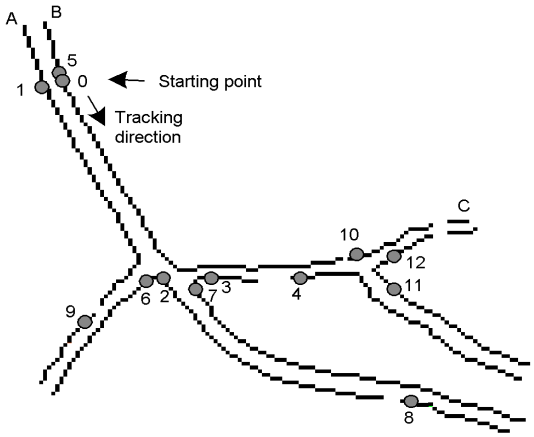

Figure 7: Example illustrating the tracking and seed generation process of the vessel tracking module

Figure 8 gives an example of tracking results on an image of our dataset. The two dark points are the two seeds at the origin of the tracking process for this image. Even with only two seeds, most of the veins have been detected. More seeds would help recover missing parts of the network.

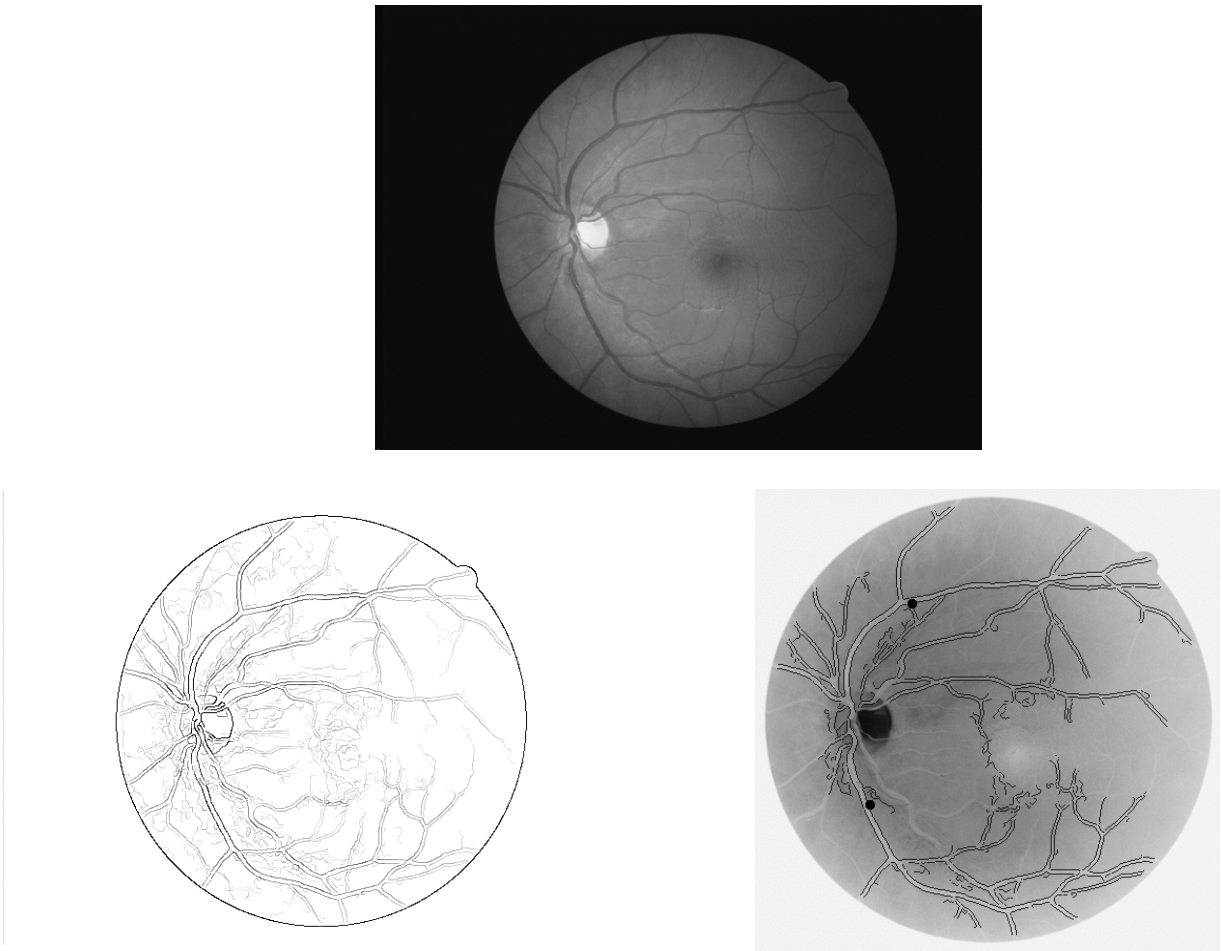

Figure 8: Example of tracking result (bottom-right) on the green band of an image of our dataset (top) based on the Canny edge detector (bottom-left).

Up to now, the algorithm has been tested on five images of our dataset with results similar to the above. It is difficult however to quantify the performance since establishing a grown truth of the vascular network is highly subjective.

7. CONCLUSION

We have presented an overview of a generic procedure for the detection of all important anatomical structures in color retinal images: the optic disk, the macula and the retinal network. The procedure has been tested on a database of 40 color fundus images acquired from a low resolution digital non-mydriatic fundus camera.

Test results show robustness against visual quality of the images and independently on the fact that the acquisition is macula- or optic disk-centered. Success rates of 100% is reached for the optic disk detection and 95% for the macula detection. We are currently working on the design of a quantitative measure protocol to help establishing the performance of the vascular network extractor.

Future works include other extensive tests on other types of fundus images acquired from different digital cameras. Algorithms will certainly have to be modified in order to keep the detection performance to the current level.

Finally, we currently use the above procedure as a preprocessing step for the development of lesions detection algorithms associated to diabetic retinopathy and other retinal diseases.

REFERENCES

1. B. Kochner, D. Schuhmann, M. Michaelis, G. Mann, K.-H. Englmeier, "Course tracking and contour extraction of retinal vessels from color fundus photographs: Most efficient use of steerable filters for model-based image analysis", in *Medical Imaging 1998: Image Processing*, Kenneth M. Hanson, Editor, Proceedings of SPIE Vol. 3338, 755-761, 1998.
2. V. Rakotomalala, L. Macaire, J-G. Postaire, M. Valette, "Identification of retinal vessels by color image analysis", *Machine Graphics and Vision*, **7**, 725-742, 1998.
3. L. Gagnon, "Rapport d'avancement Patrimoine VAI", Report CRIM-00/06-04, ISBN-2-921316-64-1, May 2000
4. M. Beaulieu, "Algorithme de détection de la macula sur les images de la bande verte de la rétine à l'aide de la technique des ondelettes pyramidales", Report CRIM-00/07-05, ISBN-2-89522-004-2, July 2000
5. F. Zana, J.-C. Klein, "A multimodal registration algorithm of eye fundus images using vessels detection and Hough transform", *IEEE Trans. Medical Imaging*, **18**, 419-428, 1999
6. P. H. Gregson, Z. Shen, R.C. Scott, V. Kozousek, "Automated grading of venous beading", *Computers and Biomedical Research*, **28**, 291-304, 1995
7. L. Pedersen, M. Grunkin, B. Ersbøll, K. Madsen, M. Larsen, N. Christoffersen, U. Skands, "Quantitative measurement of changes in retinal vessel diameter in ocular fundus images", *Patt. Recog. Lett.*, **21**, 1215-1223, 2000
8. M. Lalonde, L. Gagnon, M. C. Boucher, "Automatic image quality assessment in optical fundus images", CRIM Report CRIM-00/12-11, ISBN-2-89522-006-9, Dec. 2000
9. M. Lalonde, M. Beaulieu, L. Gagnon, "Fast and robust optic disk detection using pyramidal decomposition and Hausdorff-based template matching", Report CRIM-00/12-10, ISBN 2-89522-005-0, Dec. 2000
10. M. Lalonde, L. Gagnon, M.-C. Boucher, "Non-recursive paired tracking for vessel extraction from retinal images", *Proceedings of the Conference Vision Interface 2000*, 61-68, 2000
11. S. C. Lee, Y. Wang, "Automatic retinal image quality assessment and enhancement", in *Medical Imaging 1999: Image Processing*, Kenneth M. Hanson, Editor, Proceedings of SPIE Vol. 3661, 1581-1590, 1999.
12. J. Hall, *Mathematical techniques in multisensor data fusion*, Artec House, New York, 1992